# XAS investigation of $Al_2O_3$-coated nano-composite $ZrO_2$

**Michael Hagelstein,[a*†] Herbert O. Moser,[a] Dieter Vollath,[a] Claudio Ferrero[b] and Michael Borowski[b]**

*[a]Forschungszentrum Karlsruhe, P. O. Box 3640, D-76021 Karlsruhe, Germany, [b]European Synchrotron Radiation Facility, B. P. 220, F-38043 Grenoble Cedex, France. Email:hagel@anka-online.com*

In order to complement the structural characterisation by high resolution electron microscopy and perturbed angular correlation spectroscopy (PAC) of $Al_2O_3$ coated nano-composite $ZrO_2$, XAFS spectra have been acquired and analysed. The electron micrographs showed fringes of a well ordered lattice and well defined crystal faces of the as-produced powder whereas the PAC spectra indicated a strongly distorted short range order.
On the basis of the XAFS data, a structural model for the $ZrO_2$ core of the nano-composite $ZrO_2/Al_2O_3$ with a well ordered Zr lattice and a sevenfold, strongly distorted nearest neighbour oxygen shell is proposed. A smooth temperature dependence without an indication for a phase transformation up to a temperature of 700K has been revealed.

**Keywords: nano-composite, zirconia, $ZrO_2/Al_2O_3$, Zr K edge XAFS**

## 1. Introduction

Nano-particles often crystallize in different structures than bulk materials. A typical example is $ZrO_2$, crystallizing monoclinic as bulk material at room temperature. Nano-particles with sizes around 5nm are – depending on the production route - found in the cubic or tetragonal phase. $ZrO_2/Al_2O_3$ coated nano-particles were prepared by the microwave plasma process. This synthesis method allows the production of nanocrystalline particles with core and coating in a two-step process (Vollath *et al.*, 1997). Within the range of accuracy, electron-diffraction and -microscopy revealed a possibly cubic cation lattice. The results from PAC measurements of the electric quadrupole interaction of $^{181}$Ta on Zr sites indicate a highly disordered oxygen environment of the nano-composite in the as-prepared state (Forker *et al.*, 2000). Upon annealing, an oxygen environment around Zr cations of perfect tetragonal symmetry is observed above 500K but the phase transformation to monoclinic symmetry is completely suppressed up to a temperature of 1400K. This disorder-order transformation is partially reversible. In addition, a decrease of the vibrational amplitudes with decreasing particle size was observed.
XAFS studies have been reported for zironia compounds (Tuilier *et al.*, 1987; Li *et al.*, 1993) and of zirconia particles located in grain boundaries of $\alpha$-alumina (Loudjani and Cortes, 1997).

## 2. Experimental

The nano-crystalline $ZrO_2/Al_2O_3$ (particle size approximately 5nm) and the coarse-grain, cubic stabilised reference material $ZrO_2$:$Y_2O_3$ (20mol% $Y_2O_3$ used as obtained) was mixed with BN to form a homogeneous powder and subsequently pressed to a pellet.
The XAFS experiments have been performed on BM29 at the European Synchrotron Radiation Facility. A Si(311) double crystal monochromator has been used with the 2nd crystal detuned for harmonic suppression. An energy range 17.75keV to 19.0keV has been measured. The spectra were calibrated setting the maximum inflection point of the Zr K edge of $ZrO_2$ to 17.998keV.

## 3. Results

### *3.1 X-ray Absorption Near Edge Structure (XANES)*

The fine structure at threshold of the reference compound and the nano-composite $ZrO_2/Al_2O_3$ at room temperature is displayed in Fig. 1. The general XANES features of the nano-composite and the reference compound are similar indicating that the overall structure is similar. A strong shoulder at 17.997keV is observed which is attributed to a 1s→4d transition. This feature is strong in compounds with a non-centrosymmetric Zr environment (Li *et al.*, 1993). A characteristic splitting of the first peak at 18.003keV is observed for the yttria stabilised reference compound whereas this feature is smeared for the nano-composite.

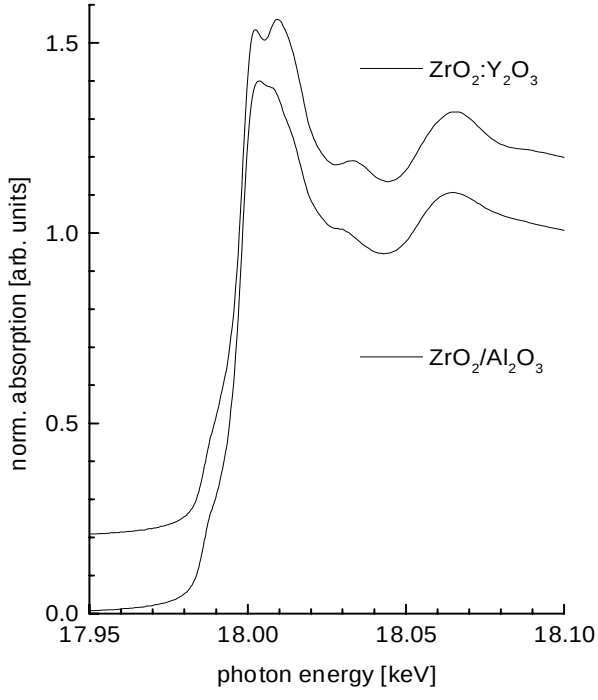


**Figure 1**
Normalised spectra at room temperature at threshold of $ZrO_2/Al_2O_3$ nano-composite (lower) and the $ZrO_2$:$Y_2O_3$ reference compound (upper, shifted by a constant offset of 0.2).

† current address: ANKA GmbH c/o Forschungszentrum Karlsruhe, Hermann-von-Helmholtz-Platz 1, D-76344 Karlsruhe

  

### 3.2 Extended X-ray Absorption fine structure (EXAFS)

The EXAFS amplitude of $ZrO_2/Al_2O_3$ nano-composite above the edge appears to be damped compared to the coarse grain $ZrO_2$:$Y_2O_3$ stabilised reference compound (Fig. 2). The EXAFS was analysed using established methods. Deviation from a Gaussian pair distribution function is accounted for by the application of the cumulant expansion. The data analysis program WinXAS (Ressler, 1998) has been used. Theoretical phase and backscattering functions which have been calculated using the multiple scattering code FEFF (Mustre de Leon *et al.*, 1991) on the basis of model compounds are included.

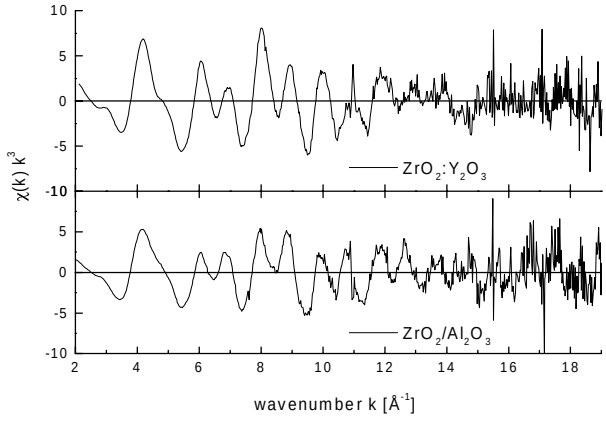


**Figure 2**
Weighted EXAFS $\chi(k)\ k^3$ of $ZrO_2/Al_2O_3$ nano-composite (lower) and the $ZrO_2$:$Y_2O_3$ stabilised reference compound (upper).

A refinement of the experimental data to the EXAFS formula including the 3rd cumulant parameter and using the calculated FEFF functions has been performed. After Fourier transformation over a wavenumber range k 2.5Å$^{-1}$ to 14Å$^{-1}$ and a Bessel window, each shell has been fitted individually in R space (see Fig. 3). For both the nano-composite and the yttria stabilised $ZrO_2$, the first prominent peak at 1.7Å can be fitted using a single Zr-O shell, the prominent peak at 3.3Å by a single Zr-Zr shell. Two further peaks at larger distances (4.77Å and 6.77Å) are remarkably stronger for the nano-composite than for the yttria stabilised compound. These intense next-nearest neighbour scattering signals have been reported to appear due to multiple scattering specifically for the tetragonal structure of $ZrO_2$ because of colinear arrays of the cation lattice (Li *et al.*, 1993). The fit results are summarised in table 1.

**Table 1**
Result of the EXAFS refinement of the 2 prominent peaks in the Fourier transform FT($\chi$(k)k$^3$) of the nano-composite $ZrO_2/Al_2O_3$ and of the reference compound $ZrO_2$:$Y_2O_3$.

| | *$ZrO_2/Al_2O_3$* | | *$ZrO_2$:$Y_2O_3$* | |
|---|---|---|---|---|
| Shell | Zr-O | Zr-Zr | Zr-O | Zr-Zr |
| Distance R [Å] | 2.14 | 3.65 | 2.19 | 3.60 |
| coordination No N | 4.1 | 6.4 | 5.4 | 10.5 |
| $\sigma^2$ [Å$^2$ * 10$^3$] | 5.8 | 8.0 | 7.6 | 10.1 |
| $\Delta E_0$ [eV] | -1.5 | -1.4 | -1.1 | -3.4 |
| 3rd cumulant [*10$^3$] | 0.8 | 0.2 | 1.0 | 0.2 |

The coordination numbers for the nano-composite $ZrO_2/Al_2O_3$ are damped due to the finite crystal size. Compared to the coarse-grained $ZrO_2$:$Y_2O_3$ reference compound, the nano-composite exhibits smaller coordination numbers for both shells. The Zr-O shell distance is shorter, the Zr-Zr distance longer than for $ZrO_2$:$Y_2O_3$. It cannot be excluded that the coordination numbers are too small due to interference of closely lying shells. An EXAFS refinement of two closely separated Zr-O shells for $Ga_2O_3$ stabilised $ZrO_2$ has been reported (Barret and Berthet, 1997). Attempts to fit the peaks of the Fourier transform with a set of up to three Zr-O shells gave rise to coordination numbers which are closer to the crystallographic values but these results are difficult to interpret due to strong correlation of parameters and are not discussed in further depth here.

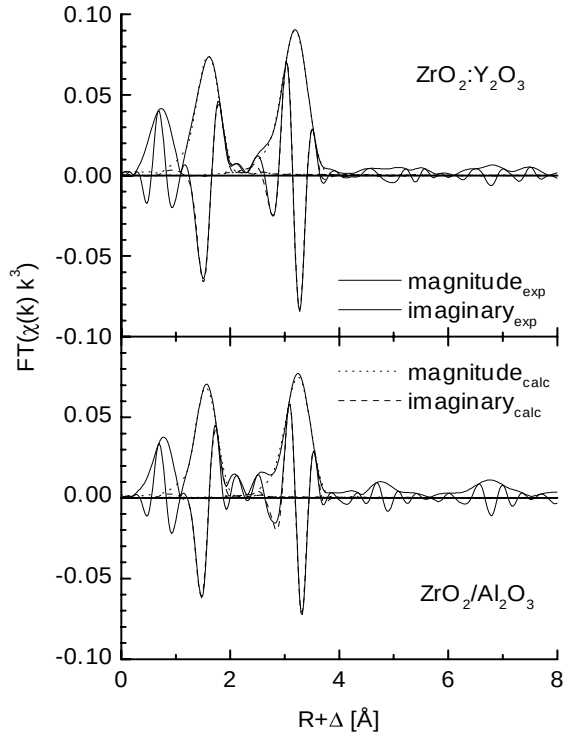


**Figure 3**
Fourier transform of the weighted $\chi(k)k^3$ of $ZrO_2$:$Y_2O_3$ (upper) and $ZrO_2/Al_2O_3$ (lower graph). Experimental data (continuous line) and fit results for the magnitude (dotted) and the imaginary part (dashed) are displayed for both the Zr-O and Zr-Zr shells.

### 3.3 Temperature dependent XAFS analysis of the nano-composite

The sample has been submitted to a temperature ramp up to a maximum temperature of 800K. XAFS spectra have been acquired at regular temperature intervals. The results of a single shell EXAFS refinement of the Zr-O shell are given in table 2. No indication for an abrupt phase transformation is observed.

**Table 2**
Results for the Zr-O shell XAFS refinement of nano-composite $ZrO_2/Al_2O_3$ at elevated temperature.

| *Temperature [K]* | *433* | *523* | *573* |
|---|---|---|---|
| Coordination number N | 4.5 | 4.6 | 4.6 |
| Distance R [Å] | 2.17 | 2.18 | 2.18 |
| $\sigma^2$ [Å$^2$ * 10$^3$] | 8.6 | 9.1 | 9.6 |
| $\Delta E_0$ [eV] | -1.3 | -1.0 | -0.9 |
| 3rd cumulant [*10$^3$] | 1.4 | 1.6 | 1.6 |

## 4. Discussion

In order to interpret the results of the refinement of the nano-composite $ZrO_2/Al_2O_3$, model calculation of the three model structures for $ZrO_2$ (cubic space group Fm3m (Antonioli *et al.*, 1994), tetragonal $P4_2/nmc$ (Inorganic Crystal Structure Database (ICSD) entry No. 4275), monoclinic $P2_1/c$ (ICSD entry No. 6184)) have been performed. Distances to neighbours up to 5.2Å and up to four leg multiple scattering paths have been taken into account. Each of the crystallographic models give rise to pronounced features in the Fourier transformed XAFS data which should serve to differentiate between them (Fig. 4).

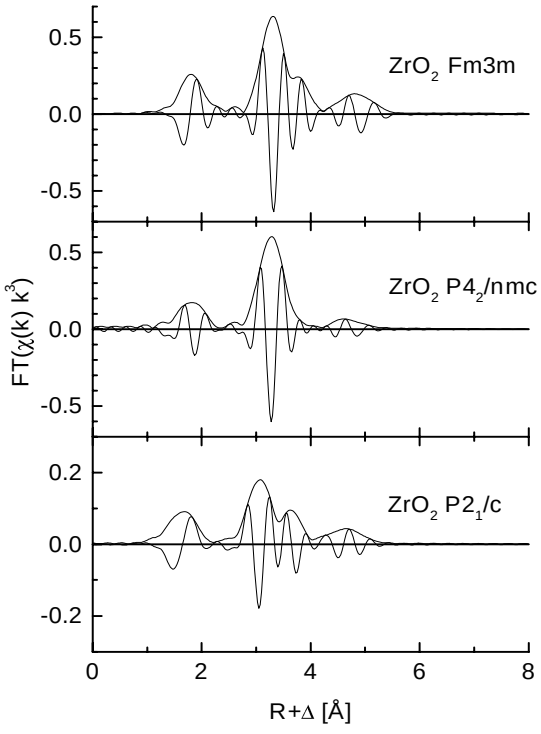


**Figure 4**
Fourier transform $FT(\chi(k)k^3)$ of FEFF model calculations for $ZrO_2$ crystallising in the different space groups cubic Fm3m, tetragonal $P4_2/nmc$ and monoclinic $P2_1/c$. Shells up to a distance of 5.2Å taken into account.

The cubic structure is composed of two discrete, nearest neighbour coordination shells Zr-O (R=2.23Å, N=8) and Zr-Zr (R=3.65Å, N=12). The high symmetry gives rise to pronounced multiple scattering at a distance of 4.47Å, leading to a shoulder of the Zr-Zr single scattering peak in the Fourier transform at $R+\Delta$=3.8Å. These two shells are split into four shells at distinctly different distances in case of the tetragonal structure ($R_{O1}$=2.07Å, $N_{O1}$=4, $R_{O2}$=2.45Å, $N_{O2}$=4, $R_{Zr1}$=3.64Å, $N_{Zr1}$=4, $R_{Zr2}$=3.68Å, $N_{Zr2}$=8). The strong splitting of the two discrete Zr-O distances leads to the double peaked feature of the imaginary part of the first prominent FT peak at $R+\Delta$=1.7Å. The differences between the tetragonal and the cubic structure is less sharp analysing the coordination in terms of average shells. The summed coordination numbers $N_a$ for the shells at averaged distances $R_a$ for Zr-O ($R_{a,O}$=2.26Å, $N_a$=8) and Zr-Zr ($R_{a,Zr}$=3.67Å, $N_a$=12) are identical to the cubic unit cell. The low monoclinic symmetry leads to a further splitting of the shells. The radial distribution function is characterised by a large number of closely spaced coordination shells leading to a strongly damped FT magnitude. The Zr-O shell is composed of 7 oxygen atoms scattered at radial distances between 2.05Å to 2.28Å with a mean distance $R_a$ of 2.16Å, the nearest neighbour Zr shell is composed of 12 Zr atoms at distances extensively scattered from 3.33Å to 4.03Å ($R_{a,Zr}$=3.81Å, $N_a$=12).

The experimental Fourier transformed $FT(\chi(k)k^3)$ of the nano-composite $ZrO_2/Al_2O_3$ and the $ZrO_2$:$Y_2O_3$ reference compound (see Fig. 3) does not show multiple scattering signals via intermediate oxygen atoms. This absence rules out an eight-fold oxygen coordination of cubic symmetry. The strong splitting of two distinct Zr-O shells which should be evident in case of a tetragonal structural variety is observed neither. The measured Zr-O distance for the nano-composite is comparable to the monoclinic form of $ZrO_2$ and implies an oxygen coordination number 7, assuming a damping of the refined value due to the small crystallite dimensions.
The Zr-Zr shell of the nano-composite does not show a broad distribution of distances and a resemblance to the crystal structure of monoclinic $ZrO_2$ can be ruled out. The small coordination number may be explained by the small particle size or a partial incorporation of Zr cations into the $Al_2O_3$ shell. The nearest neighbour Zr shell signal and the signal at long distances point towards a cubic or tetragonal arrangement of cations.

## 5. Conclusions

The nano-composite $ZrO_2/Al_2O_3$ seem to crystallise in a well ordered cation lattice but with a deficiency in nearest neighbour oxygen coordination number and a stochastic occupation of non-cubic lattice positions. This model would explain the observed lattice fringes of the electron micrographs (Vollath *et al.*, 1997), the strong local disorder of the oxygen shell (Forker *et al.*, 2000) and the results of the XAFS refinement presented here.

## References

Antonioli, G., Lottici, P. P., Manzini, I., Gnappi, G., Montenero, A., Paloschi, F. and Parent, P. (1994). *Journal of Non-crystalline Solids* **177**, 179-186.
Barret, P. and Berthet, P. (1997). *J. Phys. IV France* **7**, C2-1141-C2-1142.
Forker, M., Schmidberger, J., Szabo, D. V. and Vollath, D. (2000). *Physical Review B* **61**(2), 1014-1025.
Li, P., Chen, I.-W. and Penner-Hahn, J. E. (1993). *Physical Review B* **48**(14), 10063-10073.
Loudjani, M. K. and Cortes, R. (1997). *J. Phys. IV France* **7**, C2-1209-C2-1210.
Mustre de Leon, J., Rehr, J. J., Zabinsky, S. I. and Albers, R. C. (1991). *Physical Review B* **44**, 4146-4156.
Ressler, T. (1998). *Journal of Synchrotron Radiation* **5**, 118-122.
Tuilier, M. H., Dexpert-Ghys, J., Dexpert, H. and Lagarde, P. (1987). *Journal of Solid State Chemistry* **69**, 153-161.
Vollath, D., Szabo, D. V. and Haußelt, J. (1997). *Journal of the European Ceramic Society* **17**, 1317-1324.